



Full Text View

[Volume 32, Issue 7 \(July 2002\)](#)

Journal of Physical Oceanography

Article: pp. 2020–2033 | [Abstract](#) | [PDF \(807K\)](#)

SOFAR Floats Reveal Midlatitude Intermediate North Atlantic General Circulation. Part I: A Lagrangian Descriptive View

Michel Ollitrault

Laboratoire de Physique des Océans, IFREMER Centre de Brest, Plouzané, France

Alain Colin de Verdière

Laboratoire de Physique des Océans, Université de Bretagne Occidentale, Brest, France

(Manuscript received May 15, 2000, in final form October 15, 2001)

DOI: 10.1175/1520-0485(2002)032<2020:SFRMIN>2.0.CO;2

ABSTRACT

Quasi-Lagrangian trajectories of 26 sound fixing and ranging (SOFAR) floats have been collected near a depth of 700 m in the Central North Atlantic between 1983 and 1989, aiming at studying the influence of the Mid-Atlantic ridge on the large-scale intermediate circulation. Launched as tight clusters (18 km near neighbor distance) on either side of the Mid-Atlantic ridge, the floats dispersed quickly over a few months, jumping from one mesoscale eddy to the next. By and large, cyclonic and anticyclonic eddy motions are equipartitioned. Apparently the Mid-Atlantic ridge remains a barrier even at that shallow depth, since only one float from either side drifted across the ridge. After a few years, floats have circulated through most of the western basin (west of the Mid-Atlantic ridge), between 30° and 45°N; while east of the ridge and south of the Azores Plateau, floats advected east of the Great Meteor et al. Seamounts by the Azores current wandered more sluggishly. On this timescale, float dispersion is much more efficient zonally than meridionally, an anisotropy mainly seen west of the ridge, where floats spread westward over 30° longitude, while no float penetrated south of 30°N and only two crossed 45°N northward.

1. Introduction

Although the North Atlantic Ocean is probably the best sampled of all oceans, we do not have yet a quantitative knowledge (e.g., with a 30% accuracy) of its three-dimensional general circulation. Many transoceanic hydrographic sections (e.g., those of the IGY 1957 and 1958) have

Table of Contents:

- [Introduction](#)
- [The drifter and float](#)
- [Lagrangian view of lower](#)
- [Concluding remarks](#)
- [REFERENCES](#)
- [TABLES](#)
- [FIGURES](#)

Options:

- [Create Reference](#)
- [Email this Article](#)
- [Add to MyArchive](#)
- [Search AMS Glossary](#)

Search CrossRef for:

- [Articles Citing This Article](#)

Search Google Scholar for:

- [Michel Ollitrault](#)
- [Alain Colin de Verdière](#)


elucidated the main water masses and their motions at least in a qualitative fashion. More recently inverse modeling, making use of hydrographic data with better spatial resolution and reasonable physical constraints (e.g., mass conservation) has permitted the development of a coherent picture for the mean circulation (averaged over a few square degrees in area and a few years in time), at least for the oceanic warm water sphere (i.e., the upper 1000 m or so). Since 1975, Lagrangian sound fixing and ranging (SOFAR) floats have been used to track water particles, primarily at the main thermocline depth, and for periods of a few years. These direct current measurements allow determination of absolute water velocities on meso and larger scales with unsurpassed accuracy (see for instance [Freeland et al. 1975](#); [Riser and Rossby 1983](#); [Rossby et al. 1983](#); [Owens 1991](#); [Spall et al. 1993](#); [Richardson 1993](#)).

From July 1983 to June 1989, the TOPOGULF experiment took place in the mid-North Atlantic, to obtain a better knowledge of the depth of the wind-driven circulation, and to reveal the influence of the Mid-Atlantic Ridge (MAR), whence the name TOPO (graphic) GULF (Stream). Meridional hydrographic sections were taken on both sides of the MAR between 24° and 53°N to obtain a basic description of water masses and zonal velocities. These were complemented by transverse sections, in order to have closed boxes to which one could apply conservation constraints. Four current meter arrays were also deployed near 48°N on both sides of the MAR to monitor temporal fluctuations of the North Atlantic Current (NAC) system. Various aspects of these experimental results can be found in [Arhan et al. \(1989\)](#) and [Colin de Verdière et al. \(1989\)](#).

The objectives of the Lagrangian observations (mainly SOFAR floats near 700 db) were to investigate the communications over a long period between western and eastern basins, in the vicinity of the Azores front (possibly a southern branch of the Gulf Stream), and to obtain a mean absolute velocity reference level, to be used later in conjunction with hydrography, to obtain the full circulation. The float trajectories also give insight into the mechanisms of tracer transport and dispersion.


This paper (Part I) presents the variety of mesoscale motions as revealed by individual float trajectories. Box statistics of Eulerian means and variances and horizontal diffusivity estimates are presented in a companion paper, Part II ([Ollitrault and Colin de Verdière 2002](#)).

2. The drifter and float data

In early July 1983 three surface drifters and 15 SOFAR floats were launched from the Institut Français de Recherche pour l'Exploitation de la Mer (IFREMER) R/V *Jean Charcot* within a 75-km diameter circle centered at 36°N, 40°W, west of the MAR axis, at the entrance of the Oceanographer Fracture Zone. One year later, in late October 1984, 11 more SOFAR floats were launched from Woods Hole Oceanographic Institution (WHOI) R/V *Oceanus* over a smaller, 40-km diameter area centered at 33°N, 33°W, east of the MAR axis. Finally, in mid-September 1985, the last four SOFAR floats were launched from R/V *Oceanus* near 33°N, 33°W. All floats in these three separate launchings were ballasted for 700 db. The two launching sites were chosen on the basis of XBT casts that showed the presence of a thermal front that could be related to the eastward meandering Azores current front system ([Käse et al. 1985](#); [Gould 1985](#)). Near neighbor distance between western floats (drifters) at launch was, respectively, ~ 18 and ~ 55 km. The eastern floats, however, were launched in duo or trio (two or three floats separated by ~ 2 km) with a ~ 18 km distance between groups, a launching scheme intended to provide insight into relative dispersion of fluid particles ([Fig. 1](#) .

Drifters consisted of a surface buoy fitted with a plastic sail 3 m by 10 m centered near 100-m depth. They measured water temperature at 0.5-m and 5-m depths (with an accuracy of $\pm 0.05^\circ\text{C}$) at a 40-min sampling period. Between seven and eight surface positions were provided daily by ARGOS system, as well as the temperature data.

SOFAR floats used for the TOPOGULF experiment were made of aluminum tubing (30-cm diameter, more than 7 m long, for 400-kg weight in air). These floats were ballasted before launch for a target in situ density at 700 db of 1030.4 kg m^{-3} ($T = 9.9^\circ\text{C}$, $S = 35.4$) at the western launch site and 1030.3 kg m^{-3} ($T = 10.8^\circ\text{C}$, $S = 35.5$) at the eastern site. They emitted sound signals every 12 h near 260 Hz, which were picked up by several autonomous listening stations (ALS) moored near the base of the main thermocline. Sound signal times of arrival (occasionally from more than 1000-km distance) stored in the ALSs, were used to track the SOFARs, after recovery of the listening stations. SOFAR floats also telemetered temperature (accuracy $\pm 0.05^\circ\text{C}$) and pressure (accuracy ± 10 db) averaged over 48 h, but only on alternate days. As many as 41 listening stations were moored and recovered (mean life time of the order of 18 months) over the 6-yr tracking period of the floats (July 1983–June 1989). This was made possible through cooperation and resource sharing between IFREMER and WHOI. However out of the 20 different ALS locations, only 5 to 10 were simultaneously occupied. Consequently the listening coverage was not continuous for some floats.

[Table 1](#)  summarizes the life histories of the surface drifters and of the SOFAR floats. Between July 1983 and June 1984, the three drifters totaled 640 days (7 months mean lifetime). In each of the three batches of SOFAR floats launched, one float was never heard by the listening stations. We have thus obtained 27 trajectories totaling 26 732 float days. Mean lifetimes of the 27 surviving SOFAR floats is 2.7 yr (2.4 yr for the 30 floats launched). Float positions were obtained for 22 338 days (84% of the float lives), of which 2830 days (13% of the 22 338 days) correspond to pressure outside the (600–800)-db interval.

TOPOGULF SOFAR floats were nominally ballasted for 700 db, but they systematically went deeper after launch. Twenty three floats equilibrated around $770 \pm 26(1\sigma)$ db. Three floats (#19, #47, and #58) were obviously poorly ballasted since they equilibrated near 1110, 1275, and 1750 db, respectively. The equilibrium pressure after launch of only one float (#61) is not known; however, 20 days after launch, its first measured pressure was 696 db. All floats made successful use of their sacrificial anode to rise closer to 700 db. In particular, float #19 rose from 1110 to 800 db in ~ 450 days, while float #47 rose from 1275 to 700 db in ~ 800 days, after which they remained in the (600–800)-db interval. Float #58 rose from 1750 to 1400 db only, due to its shorter lifetime of 423 days. For these three deep floats the rising rates were respectively 0.68, 0.72, and 0.83 db day⁻¹. On the contrary, float #86 sank from 800 to 2181 db during its last 66 days of life. It probably collapsed afterward (theoretical buckling pressure is 2520 db). Finally, two floats rose above 600 db at depth: float #02 steadily rose from 700 to 100 db over a period of 1100 days, and then stayed at 100 db the remaining 400 days of its life; float #15 suddenly rose to 300 db, after 600 days in the (600–800)-db interval, and remained afterward at 300 db for the last 150 days of its life.

SOFAR floats were tracked by a least squares minimization over the distances between a given float and the listening stations obtained by multiplying the times of propagation by estimated mean sound speeds. Mean sound speeds were estimated from historical hydrography (Levitus 1982) with a ray-tracing program. Absolute position accuracy (based on least square residuals and differences between launch and first estimated positions) is estimated to be of the order of a few kilometers for most of the SOFAR float trajectories. Raw positions were then Lanczos filtered (periods shorter than 2 days were removed, periods greater than 5 days preserved), and cubic spline interpolated to fill gaps smaller than 5 days and to estimate velocities every 12 h.

Surface drifter ARGOS raw positions (ARGOS position accuracy is of the order of 500 m at best) were similarly filtered (periods shorter than one day were removed, periods greater than two days preserved) and splined to estimate velocities every 6 h. More details on the experiment, data processing and data itself are given in Ollitrault (1994).

3. Lagrangian view of lower thermocline motions

Trajectories from the 26 SOFAR floats in the (600–800)-db interval are shown in Fig. 2. A 9-month long trajectory (May 1985 to February 1986) from a companion experiment named NOAMP (Ollitrault et al. 1988) is also plotted (red curve near 50°N, 20°W), since this float was near the same depth (900–800 db). Figure 3 shows instead upper thermocline motions revealed by the drifter trajectories (100-db nominal depth) and SOFAR #02 (pink) and #15 (green) trajectories when they happened to be in the (100–300)-db interval.

a. Initial dispersion


1) WESTERN CLUSTER

After 120 days (Fig. 4), nine floats of the western cluster were still trapped within a cyclonic cold-core (1.6°C negative temperature anomaly at 770 db) eddy of roughly 100-km diameter (five peripheral floats were ejected about 10 days after deployment). The eddy rotation rate varies as $1/r$ (rotation period is 30 days at $r = 55$ km, near the periphery and 15 days at $r = 27.5$ km). This implies a nearly constant azimuthal velocity over radius. Unfortunately no float sampled the eddy center and a full radial velocity profile is not available. We may conjecture a solid body rotation within 10–20 km of eddy center. The eddy is intensified expectedly in the upper thermocline (near 100 m) since drifter #2112 imbedded in the same vortex swirled cyclonically with a 6-day period at $r = 27.5$ km.




After 6 months, all floats from the western cluster were wandering independently, except for one pair (floats #13 and #14), which separated a few weeks later. Nearly all floats were seeded in the cold-core cyclonic eddy except the two southernmost ones (#04 and #05) that were presumably on the edge of a warm-core anticyclonic eddy (confirmed by the surface trajectories). Furthermore we have indication of a second anticyclone (near 36°N, 38°W) east of the main cyclone (see red drifter in Fig. 3 and float #06 in Fig. 4). There are also hints of a second cyclone center near 33°N, 42°W. The Lagrangian particles behave as if they were going from one eddy of one sign to another of opposite sign, swirling at times within a given eddy for up to 6 months, being rapidly ejected at other times according to their distance from the eddy center. Note that this eddy field is not stationary: the well-sampled cold-core eddy moved slowly southwestward, parallel to the MAR about 150 km in 3 months (a 2 cm s^{-1} translational speed 10 times smaller than eddy swirl speeds), then northward back to its original latitude in 2 months.

2) EASTERN CLUSTER


The six SOFARs of the first launch, which settled in the (600–800) db interval (Fig. 5) were entrained coherently within an eastward meandering jet ($8\text{--}9 \text{ cm s}^{-1}$), thought to be the deep signature of the Azores Current (AC) before separating after 2 to 3 months (two floats recirculating back westward), as they approached the seamount chain (Great Meteor et al. Seamounts) extending meridionally near 28°–29°W from 30° to 35°N. Half of the floats (#50, #51, and #55)





later managed to pass east of the seamounts (actually, north of Cruiser Seamount $\sim 32^\circ\text{N}$). The three floats of the second launch (Fig. 6 ) were similarly entrained in a jet (15 cm s^{-1}) and translated eastward revealing a coherent two-month meridional oscillation over three degrees of latitude likely to be associated with the presence of the Seamount chain.



b. Complete trajectories



The overall pattern from the several years long trajectories reveals a very turbulent field of motions dominated by the mesoscale. Spatial scales appear visually similar west and east of the MAR as well as vertically (600–800 db and 100–300 db). A closer inspection reveals that floats launched in either subbasins (west or east) remained there nearly forever. Two exceptions occurred: float #04 in the western basin moved eastward to cross the MAR between 32° and 35°N , in February 1984 (see Fig. 10 ) and float #60 in the eastern basin moved westward crossing the MAR between 34° and 35°N , in June 1985. After a 4-month gap in trajectory float #60 finally reached 55°N , 45°W , 32 months after leaving 33°N , 33°W (dark green curve in Fig. 2 ). Western floats tend to occupy all space between the North American slope and the MAR but they never ventured south of 30°N . None crossed the MAR north of the Azores Plateau but float #20 may be on its way to cross the ridge near 52°N , 32°W just south of the Charlie Gibbs Fracture Zone, where the depth is greatest. Actually, recent RAFOS float trajectories (Spring 1997–Spring 1999) launched just west of the MAR between 45° and 55°N clearly demonstrate NAC flows east over the ridge from at least 50° to 53°N near 700 db (Bower et al. 2000). Between 30° and 37°N , several western floats (#03, #04, #05, #13 and #17), wandered, at times, around the ridge axis, showing large oscillations oriented mainly parallel to the ridge but also some crisscrossings, south of 35°N (Figs. 2, 7, 9, and 10 ). However all the floats (except #04) that crossed from the west eventually returned to the west. The ridge crest is 2000 m deep near 30°N but shallows progressively to 1000 m near 37°N , and this may call for topographic influence on the trajectories.

Although float #20 was entrained within the North Atlantic Current with a temperature of $\sim 5^\circ\text{C}$ near 52°N , 32°W , its track is not complete around 45°N on its way northward. Note also float #60 which wandered at the entrance of the Labrador Sea with a temperature of 4° – 5°C at 600 db, with some discontinuities of the track. These two floats probably entered into the subpolar gyre, tracing water from the Labrador Sea.

Instead of showing a “direct” flow from the Stream (heading northeastward), southeast of the Grand Banks (near 42°N , 45°W) to the NAC branch revealed by #20 at the end of its life, three floats (#20, #13 #16) revealed the presence of an eastward flow near 42°N toward the MAR, with float #13 thereafter turning north and reaching 46°N on the western flank of the MAR (Fig. 2 

Several western floats were entrained within the Gulf Stream but generally escaped after a few months. Floats #08 (Fig. 2 ) and #09 (Fig. 8 ) which crisscrossed the Gulf Stream translated westward for a short time in the northern gyre recirculation (Hogg 1992), north of 40°N between 60° and 50°W (temperatures of 6° – 8°C near 600–650 db). Actually, a majority of floats (#02, #03, #05, #06, #08, #09, #13, #14) translated westward during parts of their life in the southern recirculation gyre (Worthington 1976), (see Figs. 7, 8, and 9 ). One float (#06, see Fig. 8 ) found its way west directly from 37°N , 38°W to 36°N , 66°W in 15 months (mean westward speed 7 cm s^{-1}) but generally float trajectories were highly convoluted, being entrained within the Stream then escaping to return westward. Float #05 instead returned back east near 32°N after passing through the Corner Rise Seamounts.

After crossing into the eastern basin float #04 drifted eastward revealing a current jet at 700 m (Fig. 10 ) presumably the Azores Current. Such a jet (with meanders) centered around 33°N , and west of the Great Meteor et al. Seamount chain, also revealed by the subsequent launchings near 33°N , 33°W (Figs. 5 and 6 ) in October 1984 and September 1985 (#04 passed by this position at the end of May 1984) has been observed almost without interruption from March 1984 to March 1986. After that time all floats had left the zonal band 32° to 34°N situated between the MAR and the Seamounts.

Interestingly, floats #19 and #47, which traced Mediterranean Water for a few months (at 1100 and 1275 db, respectively) after their launchings, showed the presence of the meandering Azores Current as soon as they rose to depths shallower than 1000 db. This indicates the Azores Current may reach at most 1000 db so that its interaction with the underlying Mediterranean Water is probably weak. Beside floats #21 and #60, which recirculated westward, all other floats generally managed to pass through the seamounts (which culminate at 200–300 m depth), north of 32°N (Irving and Cruiser Seamounts) and continue eastward in the Canary Basin but with a dramatic change in the trajectories. Some floats collided with the Seamounts, while others passed through the gaps, then showing meridional oscillations (Fig. 6 ) and more generally a turbulent clustering just east of the Seamounts, between 30°N and 35°N (Fig. 10 ). East of the Seamounts, in the Madeira abyssal plain, the motions are comparatively sluggish, with apparently more homogeneous turbulence.

Although the Great Meteor et al. Seamounts affect strongly the mesoscale flow structure, we observe only few loopers related to the topography. Instead, in the western basin cyclonic cold-core loops were observed several times in the Corner Rise Seamounts area. Taking the Richardson (1993) definition of two or more consecutive loops to characterize a looping float trajectory, we observed several cyclonic cold-core and anticyclonic warm core loopers in both basins. Apart from the trapping in the initial cold core ring, floats were not generally entrained for more than two or three loops within swirling

eddies. It is as if floats kept wandering along the edges of eddies. For example float #21 (Fig. 2 ●) passed from a warm anticyclone (three loops) to a cold cyclone (four loops). Note also the south west drift, parallel to the MAR axis, of this cyclone, similar to the drift of the initial cyclonic eddy, which shows the MAR may act as a barrier for mesoscale motions. As a second example, float #57 (from NOAMP, see Fig. 2 ●) passed from a cold cyclone (two loops) to a warm anticyclone (three loops). A notable exception is provided by float #09 (Figs. 2 and 8 ●), which swirled cyclonically (three loops near 37°N 48°W, then three other loops south of Corner Rise Seamounts) before being trapped in a coherent anticyclonic warm-core eddy (temperature ~ 14°C at 700 db, swirl speed (~ 20 cm s⁻¹) drifting westward at a speed of about 5 km day⁻¹ between 59° and 67°W along 31.5°N. All cyclones mapped by floats were cold and all anticyclones warm.

Overall (besides meandering jets such as the Gulf Stream or Azores Current) the image of an ocean thermocline populated with as much cold-core cyclones as warm-core anticyclones seems well sustained by our float data.

By way of contrast with the zonal extension of the lower thermocline trajectories, near surface (100, 300)-db trajectories reveal large-scale motions, which are more meridionally oriented. Although the database is limited, a blocking effect of the MAR is even suggested by the upper-level trajectories of Fig. 3 ●: none of the 100-m drifters crossed the MAR. However, float #02 crossed eastward near 300-m depth and around 33°N, revealing the Azores Current until it got entangled in the Great Meteor et al. Seamounts. Its general motion thereafter at depths between 200 and 100 m was consistent with the general wind-driven anticyclonic gyre circulation. [Sundermeyer and Price \(1998\)](#) show similar 300 m float trajectories in this region around 25°N, 28°W.

c. Net displacements

Displacements of the western floats are shown after 6, 12, 18, and 24 months from initial positions in Fig. 11 ●. If we had a great number of floats seeded at the same time in the launching area such diagrams would give us an image of the evolution of the cloud of particles, enabling us to calculate tracer concentration. We have only 14 floats at the west site, 6 and 3 at the east site. Let us concentrate first on the western cluster dispersion.

Far from showing coherent tongues of marked fluids as would be the case for an underlying large-scale, slowly evolving general circulation, the displacement diagrams give instead the impression of turbulent explosions. After the first 6 months over which floats disperse from each other, large ocean areas are being swept by the floats that behave quite independently from each other. A great sensitivity of subsequent displacements (after one or two years) to initial conditions is the rule and confirms that the underlying velocity field is of a turbulent nature. A statistical quantification (the so-called one-particle diffusivities) of this long-term chaotic behavior will be given in Part II. Although the float scatter at relatively small time (6 months) looks roughly isotropic, it is particularly obvious that the long term behavior of the western cluster after two years favors zonal over meridional displacements. Away from western boundary currents, we may hypothesize that the β -effect is active at low frequencies to restore fluid parcels near their starting latitudes (again the large time behavior of the one-particle diffusivities will allow us to quantify this). Things are less clear for the two eastern clusters, although zonal dispersion also seems to prevail over meridional in the long term (but we have very few floats).

Over the total duration of the experiment, the Lagrangian mean velocity, defined as the displacement averaged over all the floats of a given cluster, is a westward flow for the western cluster (speed 1.0 cm s⁻¹ toward 285°) and a southeastward flow for the eastern clusters (speed 0.5 cm s⁻¹ toward 135°). This answers one objective of the experiment, namely “the exploration of the degree of flow communication across the MAR”: the Lagrangian mean flow near 700 m diverges “away” from the ridge. Therefore, although some communication between the two basins for these particular launch sites is not excluded, we conclude that this communication occurs with rather low probability and that the thermocline water mass characterizing this 10°C water appears to mix predominantly within each subbasin. Whether it is large scale topography or other dynamical constraint, which is responsible for this lack of communication is an open question.

4. Concluding remarks

The quasi-Lagrangian character of the trajectories of the 26 SOFAR floats launched at the base of the North Atlantic subtropical gyre, as part of the TOPOGULF experiment, gives the destination of fluid parcels initially on either sides of the MAR. After nearly 3 years, floats have occupied the whole width of the subtropical gyre, from 30° to 45°N, west of the MAR but only south of the Azores Plateau (at 38°N) east of the MAR. The invasion of the gyre occurs mainly by random jumping from one mesoscale eddy to the next (cold cyclones or warm anticyclones).

This broad brush picture, however, conceals the fact that only one of the floats of each cluster managed to cross the MAR, which is therefore a very strong barrier to flows well above: the Lagrangian mean flow diverges from the crest of the MAR; there are several examples of eddies that drift parallel to the MAR axis.

A second barrier is the 30°N latitude (only in the Canary Basin a few floats wandered south of it). Since [Dantzler's \(1977\)](#) map shows a strong drop of eddy potential energy at this latitude, this suggests that float invasion from the north does not occur because of a weakness of eddy activity south of 30°N. Besides the weak Canary Basin southern escape (east of the Great Meteor et al. Seamount chain), the experiment reveals a second possible escape towards the subpolar gyre, between the western boundary and the MAR, north of 45°N. Only one float however proceeded to the North East within the North Atlantic Current.

The float clusters were launched on the presumed path of the Azores Current, both east and west of the MAR, but instead of revealing steady eastward advection, they suffered turbulent explosions, isotropic at small times, becoming later anisotropic (after one year or more) with dominant excursion in the zonal direction (this agrees with an aspect ratio of zonal over meridional sizes of the domain of invasion of about 2). However, meandering eastbound Azores Current jets were revealed by several floats (down to 1000 m), between the MAR and the Great Meteor et al. Seamounts. Downstream (east) of the seamounts, meridional oscillations reaching 5° latitude at times, appear and are the likely results of the interaction of the Azores Current with the seamounts.

Acknowledgments

The floats were expertly designed by Doub Webb and carefully prepared by Pierre Tillier. Isabelle Bodevin and Daniel Gouriou helped a lot to develop the tracking software, Patrice Caprais, Jean-Philippe Rannou, and Richard Schopp to track the floats. We also thank all the persons that have helped to make this float project successful and we gratefully acknowledge the continued support of IFREMER throughout the years. We had fruitful discussions with Phil Richardson during the final writing of the paper.

REFERENCES

- Arhan M., A. Colin de Verdière, and H. Mercier, 1989: Direct observations of the mean circulation at 48°N in the Atlantic Ocean. *J. Phys. Oceanogr.*, **19**, 161–181. [Find this article online](#)
- Bower A., Coauthors, 2000: Warm-water pathways in the subpolar North Atlantic: An overview of the ACCE RAFOS float programme. *WOCE Int. Newslett.*, **38**, 14–16. [Find this article online](#)
- Colin de Verdière A., H. Mercier, and M. Arhan, 1989: Mesoscale variability transition from the western to the eastern Atlantic along 48° N. *J. Phys. Oceanogr.*, **19**, 1149–1170. [Find this article online](#)
- Dantzler H. L., 1977: Potential energy maxima in the tropical and subtropical North Atlantic. *J. Phys. Oceanogr.*, **7**, 512–519. [Find this article online](#)
- Freeland H. J., P. B. Rhines, and T. Rossby, 1975: Statistical observations of the trajectories of neutrally buoyant floats in the North Atlantic. *J. Mar. Res.*, **33**, 383–404. [Find this article online](#)
- Gould W. J., 1985: Physical oceanography of the Azores front. *Progress in Oceanography*, Vol. 14, Pergamon, 167–190.
- Hogg N., 1992: On the transport of the Gulf Stream between Cape Hatteras and the Grand Banks. *Deep-Sea Res.*, **39**, 1231–1246. [Find this article online](#)
- Käse R. H., W. Zenk, T. B. Sanford, and W. Hiller, 1985: Currents, fronts and eddy fluxes in the Canary Basin. *Progress in Oceanography*, Vol. 14, Pergamon, 231–257.
- Levitus S., 1982: *Climatological Atlas of the World Ocean*. NOAA Prof. Paper 13, 173 pp. and 17 microfiche.
- Ollitraul M., 1994: The TOPOGULF Experiment Lagrangian data. *Repères Océan*, No. 7, IFREMER, 622 pp.
- Ollitraul M., and A. Colin de Verdière, 2002: SOFAR floats reveal midlatitude intermediate North Atlantic general circulation. Part II: An Eulerian statistical view. *J. Phys. Oceanogr.*, **32**, 2034–2053. [Find this article online](#)
- Ollitraul M., P. Tillier, I. Bodevin, and H. Klein, 1988: Deep SOFAR float experiment in the northeast Atlantic. *Rapports Sci. Technol.*, No. 11, IFREMER, 122 pp.
- Owens W. B., 1991: A statistical description of the mean circulation and eddy variability in the northwestern Atlantic using SOFAR floats. *Progress in Oceanography*, Vol. 28, Pergamon, 257–303.
- Richardson P., 1993: A census of eddies observed in North Atlantic SOFAR float data. *Progress in Oceanography*, Vol. 31, Pergamon, 1–50.

Riser S. C., and H. T. Rossby, 1983: Quasi-Lagrangian structure and variability of the subtropical western North Atlantic circulation. *J. Mar. Res.*, **41**, 127–162. [Find this article online](#)

Rossby H. T., S. C. Riser, and A. J. Mariano, 1983: The western North Atlantic: A Lagrangian viewpoint. *Eddies in Marine Science*, A. R. Robinson, Ed., Springer-Verlag, 66–91.

Spall M. A., P. L. Richardson, and J. Price, 1993: Advection and eddy mixing in the Mediterranean salt tongue. *J. Mar. Res.*, **51**, 797–818. [Find this article online](#)

Sundermeyer M. A., and J. F. Price, 1998: Lateral mixing and the North Atlantic Tracer Release Experiment: Observations and numerical simulations of Lagrangian particles and a passive tracer. *J. Geophys. Res.*, **103**(C10), 21481–21497. [Find this article online](#)

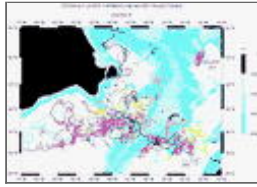
Worthington L. V., 1976: *On the North Atlantic Circulation*. Vol. 6. *The Johns Hopkins Oceanographic Studies*, 110 pp.

Tables

TABLE 1a. Summary of 700-dbar SOFAR float data

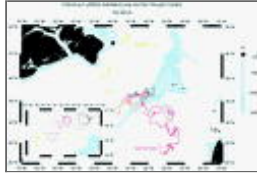
Year	Launch position and date	First pressure and temperature	Pressure and temperature range	Final pressure and date	Final temperature and date	Rad position	Number of days from launch to end of profile	Western Basin number of days tracked within 1000–9000 bar	Corresponding number of days pressure and temperature	Eastern Basin number of days tracked within 1000–9000 bar	Corresponding number of days pressure and temperature
10	37°11'N 74°14'W	700 dbar	60–700 dbar	27°14'N 74°14'W	27.14°N 74.14°W	100.13	411.0	401.0	401.0 ± 2.0 dbar	10.0	10.0 ± 1.0 dbar
10	37°10'N 74°15'W	700 dbar	60–700 dbar	27°13'N 74°15'W	27.13°N 74.15°W	100.13	411.0	401.0	401.0 ± 2.0 dbar	10.0	10.0 ± 1.0 dbar
10	37°09'N 74°16'W	700 dbar	60–700 dbar	27°12'N 74°16'W	27.12°N 74.16°W	100.13	411.0	401.0	401.0 ± 2.0 dbar	10.0	10.0 ± 1.0 dbar
10	37°08'N 74°17'W	700 dbar	60–700 dbar	27°11'N 74°17'W	27.11°N 74.17°W	100.13	411.0	401.0	401.0 ± 2.0 dbar	10.0	10.0 ± 1.0 dbar
10	37°07'N 74°18'W	700 dbar	60–700 dbar	27°10'N 74°18'W	27.10°N 74.18°W	100.13	411.0	401.0	401.0 ± 2.0 dbar	10.0	10.0 ± 1.0 dbar
10	37°06'N 74°19'W	700 dbar	60–700 dbar	27°09'N 74°19'W	27.09°N 74.19°W	100.13	411.0	401.0	401.0 ± 2.0 dbar	10.0	10.0 ± 1.0 dbar
10	37°05'N 74°20'W	700 dbar	60–700 dbar	27°08'N 74°20'W	27.08°N 74.20°W	100.13	411.0	401.0	401.0 ± 2.0 dbar	10.0	10.0 ± 1.0 dbar
10	37°04'N 74°21'W	700 dbar	60–700 dbar	27°07'N 74°21'W	27.07°N 74.21°W	100.13	411.0	401.0	401.0 ± 2.0 dbar	10.0	10.0 ± 1.0 dbar
10	37°03'N 74°22'W	700 dbar	60–700 dbar	27°06'N 74°22'W	27.06°N 74.22°W	100.13	411.0	401.0	401.0 ± 2.0 dbar	10.0	10.0 ± 1.0 dbar
10	37°02'N 74°23'W	700 dbar	60–700 dbar	27°05'N 74°23'W	27.05°N 74.23°W	100.13	411.0	401.0	401.0 ± 2.0 dbar	10.0	10.0 ± 1.0 dbar
10	37°01'N 74°24'W	700 dbar	60–700 dbar	27°04'N 74°24'W	27.04°N 74.24°W	100.13	411.0	401.0	401.0 ± 2.0 dbar	10.0	10.0 ± 1.0 dbar
10	37°00'N 74°25'W	700 dbar	60–700 dbar	27°03'N 74°25'W	27.03°N 74.25°W	100.13	411.0	401.0	401.0 ± 2.0 dbar	10.0	10.0 ± 1.0 dbar
10	36°59'N 74°26'W	700 dbar	60–700 dbar	27°02'N 74°26'W	27.02°N 74.26°W	100.13	411.0	401.0	401.0 ± 2.0 dbar	10.0	10.0 ± 1.0 dbar
10	36°58'N 74°27'W	700 dbar	60–700 dbar	27°01'N 74°27'W	27.01°N 74.27°W	100.13	411.0	401.0	401.0 ± 2.0 dbar	10.0	10.0 ± 1.0 dbar
10	36°57'N 74°28'W	700 dbar	60–700 dbar	27°00'N 74°28'W	27.00°N 74.28°W	100.13	411.0	401.0	401.0 ± 2.0 dbar	10.0	10.0 ± 1.0 dbar
10	36°56'N 74°29'W	700 dbar	60–700 dbar	26°59'N 74°29'W	26.99°N 74.29°W	100.13	411.0	401.0	401.0 ± 2.0 dbar	10.0	10.0 ± 1.0 dbar
10	36°55'N 74°30'W	700 dbar	60–700 dbar	26°58'N 74°30'W	26.98°N 74.30°W	100.13	411.0	401.0	401.0 ± 2.0 dbar	10.0	10.0 ± 1.0 dbar
10	36°54'N 74°31'W	700 dbar	60–700 dbar	26°57'N 74°31'W	26.97°N 74.31°W	100.13	411.0	401.0	401.0 ± 2.0 dbar	10.0	10.0 ± 1.0 dbar
10	36°53'N 74°32'W	700 dbar	60–700 dbar	26°56'N 74°32'W	26.96°N 74.32°W	100.13	411.0	401.0	401.0 ± 2.0 dbar	10.0	10.0 ± 1.0 dbar
10	36°52'N 74°33'W	700 dbar	60–700 dbar	26°55'N 74°33'W	26.95°N 74.33°W	100.13	411.0	401.0	401.0 ± 2.0 dbar	10.0	10.0 ± 1.0 dbar
10	36°51'N 74°34'W	700 dbar	60–700 dbar	26°54'N 74°34'W	26.94°N 74.34°W	100.13	411.0	401.0	401.0 ± 2.0 dbar	10.0	10.0 ± 1.0 dbar
10	36°50'N 74°35'W	700 dbar	60–700 dbar	26°53'N 74°35'W	26.93°N 74.35°W	100.13	411.0	401.0	401.0 ± 2.0 dbar	10.0	10.0 ± 1.0 dbar
10	36°49'N 74°36'W	700 dbar	60–700 dbar	26°52'N 74°36'W	26.92°N 74.36°W	100.13	411.0	401.0	401.0 ± 2.0 dbar	10.0	10.0 ± 1.0 dbar
10	36°48'N 74°37'W	700 dbar	60–700 dbar	26°51'N 74°37'W	26.91°N 74.37°W	100.13	411.0	401.0	401.0 ± 2.0 dbar	10.0	10.0 ± 1.0 dbar
10	36°47'N 74°38'W	700 dbar	60–700 dbar	26°50'N 74°38'W	26.90°N 74.38°W	100.13	411.0	401.0	401.0 ± 2.0 dbar	10.0	10.0 ± 1.0 dbar
10	36°46'N 74°39'W	700 dbar	60–700 dbar	26°49'N 74°39'W	26.89°N 74.39°W	100.13	411.0	401.0	401.0 ± 2.0 dbar	10.0	10.0 ± 1.0 dbar
10	36°45'N 74°40'W	700 dbar	60–700 dbar	26°48'N 74°40'W	26.88°N 74.40°W	100.13	411.0	401.0	401.0 ± 2.0 dbar	10.0	10.0 ± 1.0 dbar
10	36°44'N 74°41'W	700 dbar	60–700 dbar	26°47'N 74°41'W	26.87°N 74.41°W	100.13	411.0	401.0	401.0 ± 2.0 dbar	10.0	10.0 ± 1.0 dbar
10	36°43'N 74°42'W	700 dbar	60–700 dbar	26°46'N 74°42'W	26.86°N 74.42°W	100.13	411.0	401.0	401.0 ± 2.0 dbar	10.0	10.0 ± 1.0 dbar
10	36°42'N 74°43'W	700 dbar	60–700 dbar	26°45'N 74°43'W	26.85°N 74.43°W	100.13	411.0	401.0	401.0 ± 2.0 dbar	10.0	10.0 ± 1.0 dbar
10	36°41'N 74°44'W	700 dbar	60–700 dbar	26°44'N 74°44'W	26.84°N 74.44°W	100.13	411.0	401.0	401.0 ± 2.0 dbar	10.0	10.0 ± 1.0 dbar
10	36°40'N 74°45'W	700 dbar	60–700 dbar	26°43'N 74°45'W	26.83°N 74.45°W	100.13	411.0	401.0	401.0 ± 2.0 dbar	10.0	10.0 ± 1.0 dbar
10	36°39'N 74°46'W	700 dbar	60–700 dbar	26°42'N 74°46'W	26.82°N 74.46°W	100.13	411.0	401.0	401.0 ± 2.0 dbar	10.0	10.0 ± 1.0 dbar
10	36°38'N 74°47'W	700 dbar	60–700 dbar	26°41'N 74°47'W	26.81°N 74.47°W	100.13	411.0	401.0	401.0 ± 2.0 dbar	10.0	10.0 ± 1.0 dbar
10	36°37'N 74°48'W	700 dbar	60–700 dbar	26°40'N 74°48'W	26.80°N 74.48°W	100.13	411.0	401.0	401.0 ± 2.0 dbar	10.0	10.0 ± 1.0 dbar
10	36°36'N 74°49'W	700 dbar	60–700 dbar	26°39'N 74°49'W	26.79°N 74.49°W	100.13	411.0	401.0	401.0 ± 2.0 dbar	10.0	10.0 ± 1.0 dbar
10	36°35'N 74°50'W	700 dbar	60–700 dbar	26°38'N 74°50'W	26.78°N 74.50°W	100.13	411.0	401.0	401.0 ± 2.0 dbar	10.0	10.0 ± 1.0 dbar
10	36°34'N 74°51'W	700 dbar	60–700 dbar	26°37'N 74°51'W	26.77°N 74.51°W	100.13	411.0	401.0	401.0 ± 2.0 dbar	10.0	10.0 ± 1.0 dbar
10	36°33'N 74°52'W	700 dbar	60–700 dbar	26°36'N 74°52'W	26.76°N 74.52°W	100.13	411.0	401.0	401.0 ± 2.0 dbar	10.0	10.0 ± 1.0 dbar
10	36°32'N 74°53'W	700 dbar	60–700 dbar	26°35'N 74°53'W	26.75°N 74.53°W	100.13	411.0	401.0	401.0 ± 2.0 dbar	10.0	10.0 ± 1.0 dbar
10	36°31'N 74°54'W	700 dbar	60–700 dbar	26°34'N 74°54'W	26.74°N 74.54°W	100.13	411.0	401.0	401.0 ± 2.0 dbar	10.0	10.0 ± 1.0 dbar
10	36°30'N 74°55'W	700 dbar	60–700 dbar	26°33'N 74°55'W	26.73°N 74.55°W	100.13	411.0	401.0	401.0 ± 2.0 dbar	10.0	10.0 ± 1.0 dbar
10	36°29'N 74°56'W	700 dbar	60–700 dbar	26°32'N 74°56'W	26.72°N 74.56°W	100.13	411.0	401.0	401.0 ± 2.0 dbar	10.0	10.0 ± 1.0 dbar
10	36°28'N 74°57'W	700 dbar	60–700 dbar	26°31'N 74°57'W	26.71°N 74.57°W	100.13	411.0	401.0	401.0 ± 2.0 dbar	10.0	10.0 ± 1.0 dbar
10	36°27'N 74°58'W	700 dbar	60–700 dbar	26°30'N 74°58'W	26.70°N 74.58°W	100.13	411.0	401.0	401.0 ± 2.0 dbar	10.0	10.0 ± 1.0 dbar
10	36°26'N 74°59'W	700 dbar	60–700 dbar	26°29'N 74°59'W	26.69°N 74.59°W	100.13	411.0	401.0	401.0 ± 2.0 dbar	10.0	10.0 ± 1.0 dbar
10	36°25'N 75°00'W	700 dbar	60–700 dbar	26°28'N 75°00'W	26.68°N 75.00°W	100.13	411.0	401.0	401.0 ± 2.0 dbar	10.0	10.0 ± 1.0 dbar
10	36°24'N 75°01'W	700 dbar	60–700 dbar	26°27'N 75°01'W	26.67°N 75.01°W	100.13	411.0	401.0	401.0 ± 2.0 dbar	10.0	10.0 ± 1.0 dbar
10	36°23'N 75°02'W	700 dbar	60–700 dbar	26°26'N 75°02'W	26.66°N 75.02°W	100.13	411.0	401.0	401.0 ± 2.0 dbar	10.0	10.0 ± 1.0 dbar
10	36°22'N 75°03'W	700 dbar	60–700 dbar	26°25'N 75°03'W	26.65°N 75.03°W	100.13	411.0	401.0	401.0 ± 2.0 dbar	10.0	10.0 ± 1.0 dbar
10	36°21'N 75°04'W	700 dbar	60–700 dbar	26°24'N 75°04'W	26.64°N 75.04°W	100.13	411.0	401.0	401.0 ± 2.0 dbar	10.0	10.0 ± 1.0 dbar
10	36°20'N 75°05'W	700 dbar	60–700 dbar	26°23'N 75°05'W	26.63°N 75.05°W	100.13	411.0	401.0	401.0 ± 2.0 dbar	10.0	10.0 ± 1.0 dbar
10	36°19'N 75°06'W	700 dbar	60–700 dbar	26°22'N 75°06'W	26.62°N 75.06°W	100.13	411.0	401.0	401.0 ± 2.0 dbar	10.0	10.0 ± 1.0 dbar
10	36°18'N 75°07'W	700 dbar	60–700 dbar	26°21'N 75°07'W	26.61°N 75.07°W	100.13	411.0	401.0	401.0 ± 2.0 dbar	10.0	10.0 ± 1.0 dbar
10	36°17'N 75°08'W	700 dbar	60–700 dbar	26°20'N 75°08'W	26.60°N 75.08°W	100.13	411.0	401.0	401.0 ± 2.0 dbar	10.0	10.0 ± 1.0 dbar
10	36°16'N 75°09'W	700 dbar	60–700 dbar	26°19'N 75°09'W	26.59°N 75.09°W	100.13	411.0	401.0	401.0 ± 2.0 dbar	10.0	10.0 ± 1.0 dbar
10	36°15'N 75°10'W	700 dbar	60–700 dbar	26°18'N 75°10'W	26.58°N 75.10°W	100.13	411.0	401.0	401.0 ± 2.0 dbar	10.0	10.0 ± 1.0 dbar
10	36°14'N 75°11'W	700 dbar	60–700 dbar	26°17'N 75°11'W	26.57°N 75.11°W	100.13	411.0	401.0	401.0 ± 2.0 dbar	10.0	10.0 ± 1.0 dbar
10	36°13'N 75°12'W	700 dbar	60–700 dbar	26°16'N 75°12'W	26.56°N 75.12°W	100.13	411.0	401.0	401.0 ± 2.0 dbar	10.0	10.0 ± 1.0 dbar
10	36°12'N 75°13'W	700 dbar	60–700 dbar	26°15'N 75°13'W	26.55°N 75.13°W	100.13	411.0	401.0	401.0 ± 2.0 dbar	10.0	10.0 ± 1.0 dbar
10	36°11'N 75°14'W	700 dbar	60–700 dbar	26°14'N 75°14'W	26.54°N 75.14°W	100.13	411.0	401.0	401.0 ± 2.0 dbar	10.0	10.0 ± 1.0 dbar
10	36°10'N 75°15'W	700 dbar	60–700 dbar	26°13'N 75°15'W	26.53°N 75.15°W	100.13	411.0	401.0	401.0 ± 2.0 dbar	10.0	10.0 ± 1.0 dbar
10	36°09'N 75°16'W	700 dbar	60–700 dbar	26°12'N 75°16'W							

Oct 1984. Three more SOFARs (float numbers in blue) were launched at the eastern site on 11 Sep 1985. A total of 30 floats was launched, but one failed in each cluster. Only the launch positions of floats that returned data are given in the figure



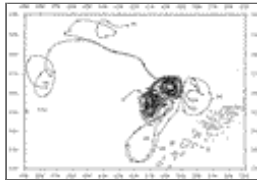
[Click on thumbnail for full-sized image.](#)

FIG. 2. All SOFAR float trajectories in the (600–800) db interval



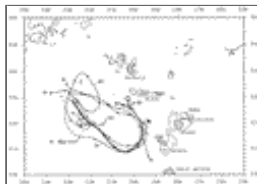
[Click on thumbnail for full-sized image.](#)

FIG. 3. Surface drifter and SOFAR trajectories in the (100–300) db interval



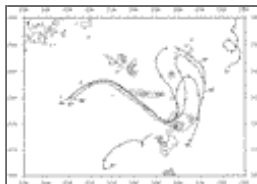
[Click on thumbnail for full-sized image.](#)

FIG. 4. First 4 months (Jul–Oct 1983) for the western cluster trajectories (14 floats). Arrowhead every 10 days. Float pair (#09 and #20) maintained a small (1–10 km) relative distance for 50 days, then separated swiftly. Another pair (#13 and #14) separated after only 6 months (in the figure these two floats are still swirling within the cold-core cyclonic eddy)



[Click on thumbnail for full-sized image.](#)

FIG. 5. First 4 months (Nov 1984–Feb 1985) for the eastern cluster (first launching). Arrowhead every 10 days. Float #60 later crossed the MAR westward. The 20 missing days at the beginning of float #61 trajectory are tentatively sketched with dashes (based on nearby trajectories)



[Click on thumbnail for full-sized image.](#)

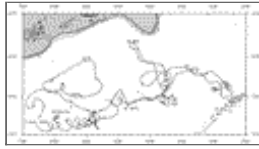
FIG. 6. First 4 months (Sep 1985–Dec 1985) for the eastern cluster (second launching). Arrowhead every 10 days. Both [Fig. 5](#) and this one show the scattering effect of the seamounts on float trajectories



[Click on thumbnail for full-sized image.](#)

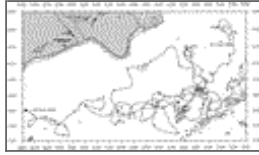
FIG. 7. Float #03 trajectory (1503 float days but positions are missing for 376 days). Arrowhead every 30 days. After wandering for more than 2 yr near its launch site, bound by the MAR in the southeast, jumping from cold (8°–9°C) cyclonic to warm

anticyclonic (10° – 11° C) eddies, it headed west to enter later into the GS (temperature 13° – 14° C) and a southern recirculation cell, completing a round trip in 9 months



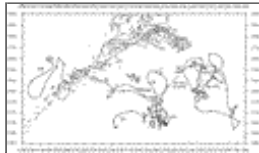
[Click on thumbnail for full-sized image.](#)

FIG. 8. Float #06 and #09 trajectories (788 float days each). Arrowhead every 30 days. While running westward, temperature gradually increases from 9° C (at launch) to 15° C in the GS



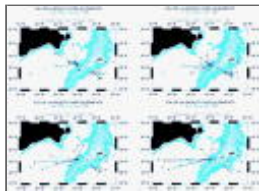
[Click on thumbnail for full-sized image.](#)

FIG. 9. Float #13 trajectory (2176 float-days but positions are missing for 240 days). Arrowhead every 30 days. After drifting westward, it returned eastward probably with the GS and was found almost back at its launch point 8 months later (on 25 Apr 1986). Thereafter it drifted west again to enter into the GS and returned near its launch point for the second time where it wandered for several months, then finally escaped northward just west of the MAR



[Click on thumbnail for full-sized image.](#)

FIG. 10. Float #04 (1804 float days) and #87 (807 float days) trajectories. Arrowhead every 30 days. There appears to be a topographic influence of the MAR on float 04 which oscillates along the H contours (f/H is similar) before crossing and flowing eastward with the Azores Current. East of 25° W, it wandered for 44 months in the Canary Basin. Float 87 launched on 11 Sep 1985 stalled east of Great Meteor Seamount then managed passing westward



[Click on thumbnail for full-sized image.](#)

FIG. 11. Western cluster float displacements after 6, 12, 18, and 24 months

Corresponding author address: Michel Ollitrault, Laboratoire de Physique des Oceans, CNRS-IFREMER, Universite, 6 avenue Le Gorgeu, BP 809, Brest Cedex, France. E-mail: Michel.Ollitrault@univ-brest.fr

top ▲



